

## Semimetallic behavior in Fe<sub>2</sub>VAl: NMR evidence

Chin-Shan Lue\* and Joseph H. Ross, Jr.†

Department of Physics, Texas A&M University, College Station, Texas 77843-4242

(Received 3 June 1998)

We report the results of a <sup>27</sup>Al and <sup>51</sup>V nuclear magnetic resonance study of Fe<sub>2</sub>VAl at temperatures between 4 and 550 K. This material has been a subject of current interest due to indications of possible heavy fermion behavior. The low-temperature NMR relaxation rate follows a Korringa law, indicating a small density of carriers at the Fermi level. At elevated temperatures, the shifts and relaxation rates go over to a thermally activated response, a semiconductorlike behavior, consistent with separate low-lying bands removed from the Fermi-level. These results are consistent with recent electronic structure calculations, and can explain both the reported activated resistivity as well as the Fermi cutoff exhibited in photoemission studies. While we observe nonstoichiometric samples of (Fe<sub>1-x</sub>V<sub>x</sub>)<sub>3</sub>Al to be magnetic, the  $x=0.33$  composition is nonmagnetic, with narrow NMR linewidths. [S0163-1829(98)07739-X]

### I. INTRODUCTION

The recently discovered nonmagnetic Heusler-type Fe<sub>2</sub>VAl alloy has attracted lots of interest because of the anomalous temperature dependence of its various physical properties. The electrical resistivity exhibits semiconducting behavior in spite of the metallic character as evidenced by photoemission.<sup>1</sup> In addition, low-temperature specific heat measurements revealed an unusual upturn in  $C/T$  with decreasing temperature, commonly observed in most heavy-fermion systems.<sup>2</sup> From the band-structure calculations, however, Fe<sub>2</sub>VAl is a semimetal with a pseudogap at the Fermi level.<sup>3-5</sup>

In this regard, it is interesting to observe whether Fe<sub>2</sub>VAl follows semiconducting or semimetal physics. Moreover, the reported resistivity and nonmagnetism for Fe<sub>2</sub>VAl are very close to those for SmB<sub>6</sub>, which has been classified as a Kondo insulator.<sup>6</sup> According to this classification, a conventional semiconductor picture is not appropriate. Hence a question which naturally arises is whether an examination of Fe<sub>2</sub>VAl will yield results similar to those in ordinary heavy fermion systems.

Nuclear magnetic resonance (NMR) is a local probe yielding information about Fermi-surface features. The NMR temperature dependence allows us to characterize the fundamental properties of Fe<sub>2</sub>VAl. In this paper, we will present NMR measurements including <sup>27</sup>Al and <sup>51</sup>V Knight shifts as well as spin-lattice relaxation rates in Fe<sub>2</sub>VAl at temperatures between 4 and 550 K. The results reveal an energy gap of 0.27 eV but with residual density of states (DOS) at Fermi level in this alloy. Thus, we provide the first experimental confirmation that the gap in Fe<sub>2</sub>VAl is actually a pseudogap, with finite carriers in the Fermi-level DOS.

### II. EXPERIMENT

The sample studied here was prepared from 99.97% Fe, 99.7% V, and 99.9% Al by mixing appropriate amounts of elemental metals, and was melted in an Ar arc furnace. The loss of weight upon melting was about 0.1% which had little effect on the NMR measurements. The resulting ingot was

annealed in a vacuum-sealed ( $10^{-5}$  torr) quartz tube at 1000 °C for 48 h, and then annealed for DO<sub>3</sub> ordering at 400 °C for 12 h followed by furnace cooling. An x-ray analysis was taken with Cu  $K\alpha$  radiation on the powder Fe<sub>2</sub>VAl. Two strong reflections could be indexed to (200) and (220) planes according to the expected DO<sub>3</sub> structure with a single weak reflection unidentified. The determined lattice parameter  $a=5.76$  Å is equal to that reported in the literature.<sup>1</sup>

The experiments were performed using a 9-T home-built pulse NMR spectrometer, described elsewhere.<sup>7</sup> The powder mixed with granular quartz was placed in a plastic vial for 4 to 300 K measurements, while we put the specimen in a Teflon tube for high temperature purposes. <sup>27</sup>Al and <sup>51</sup>V NMR spectra were thus detected around 99 and 101 MHz, respectively. The reference frequency,  $\nu_R$ , for <sup>27</sup>Al Knight shifts was the <sup>27</sup>Al resonance frequency of one molar aqueous AlCl<sub>3</sub> while the reference for <sup>51</sup>V shifts was determined from  $\nu_R \times (^{51}\gamma_n / ^{27}\gamma_n)$  with known values of  $^{27}\gamma_n = 2\pi \times 1.1093$  and  $^{51}\gamma_n = 2\pi \times 1.1193$  kHz/G.

#### A. Line shapes

Observed room-temperature powder patterns for Fe<sub>2</sub>VAl are shown in Fig. 1, measured from spin-echo integration vs. frequency. We found little line shape change with temperature. The ordered structure for this material contains an equal number of Al and V sites, both with local octahedral symmetry. For this situation, quadrupole splitting vanishes, and a single narrow line is expected for both <sup>27</sup>Al and <sup>51</sup>V, as indeed was observed. From the pulse-length dependence of the spin echo, we find that the center of both lines responds as a  $-1/2 \leftrightarrow +1/2$  central transition, while the shoulders have somewhat longer 90° pulse lengths, characteristic of satellite lines.<sup>8</sup> Thus there is a small residual quadrupole splitting, presumably due to strains in the sample.

It has been suggested that magnetic Fe atoms located on V sites may have an important role in the transport properties of Fe<sub>2</sub>VAl,<sup>3</sup> but the relatively narrow NMR line shapes place a limit on the concentration of such defects. Dipolar broadening by dilute magnetic impurities on cubic lattices can give

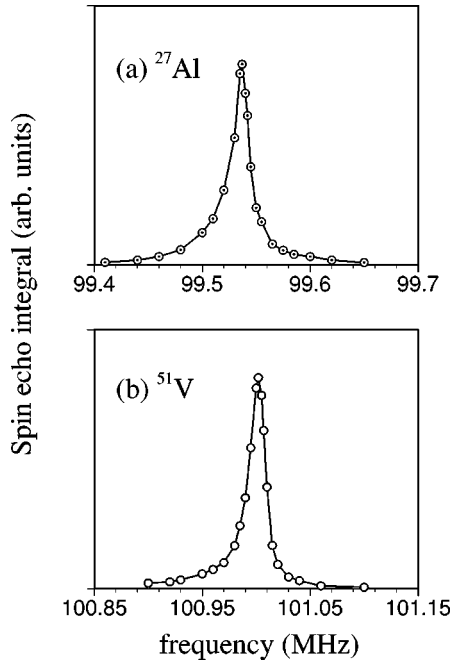


FIG. 1.  $^{27}\text{Al}$  and  $^{51}\text{V}$  NMR powder patterns in  $\text{Fe}_2\text{VAl}$  measured at room temperature.

Lorentzian line shapes.<sup>9</sup> The central portions of the transition lines (Fig. 1) do appear to have Lorentzian shapes, and a fit yielded widths (FWHM) of roughly 15 kHz and 16 kHz, for  $^{27}\text{Al}$  and  $^{51}\text{V}$ , respectively. From the theory,<sup>9</sup> the  $^{51}\text{V}$  linewidth corresponds to a maximum impurity concentration  $f = 6 \times 10^{-4}$ , for substitutional defects having a  $1 \mu_B$  moment. This concentration represents an upper limit, since some or all of the observed width could be due to quadrupole effects<sup>8</sup> or pseudoscalar splitting.

The NMR response was quite different for the case of nonstoichiometric  $(\text{Fe}_{1-x}\text{V}_x)_3\text{Al}$ , prepared in the same way as other samples. The sample with  $x=0.30$  exhibited a broad  $^{51}\text{V}$  spectrum of roughly 200 kHz FWHM at room temperature, and that with  $x=0.25$  showed even broader spectra. The NMR broadening in the nonstoichiometric compounds can be attributed to strong local magnetism. Thus, our results are in agreement with other reports<sup>1</sup> indicating that magnetism occurs for compositions other than the stoichiometric material,  $\text{Fe}_2\text{VAl}$ .

### B. Knight shifts

The Knight shifts for the stoichiometric sample were determined from the position of the maximum of each spectrum. The temperature dependences of  $^{27}\text{Al}$  and  $^{51}\text{V}$  Knight shifts, denoted as  $K_{\text{Al}}$  and  $K_{\text{V}}$ , respectively, are displayed in Fig. 2. Below 250 K, both  $K_{\text{Al}}$  and  $K_{\text{V}}$  are almost temperature independent. These constant terms originate from the orbital (paramagnetic) shifts and thus are consistent with a small contact Knight shift contribution implied by the observed long  $T_1$ 's. For the orbital shift, there is the general form<sup>10</sup>

$$\sigma^P = \frac{2e^2}{m^2 c^2} \sum \frac{\langle \Psi | L_z | \Psi' \rangle \langle \Psi' | L_z / r^3 | \Psi \rangle}{\Delta E} + \text{c.c.}, \quad (1)$$

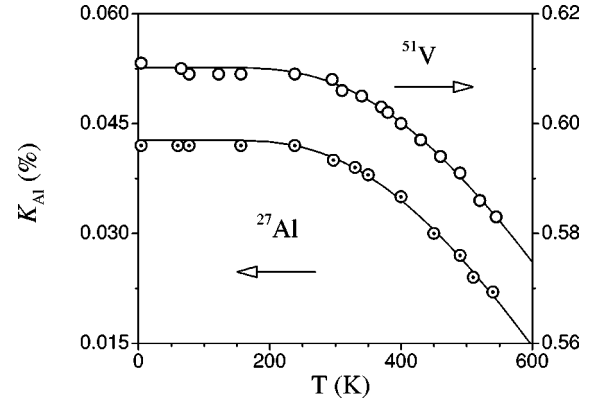


FIG. 2. Temperature dependence of observed  $^{27}\text{Al}$  and  $^{51}\text{V}$  Knight shifts. Solid curves: fits to the semiconducting behavior from Eq. (2).

where  $\Psi$  is an occupied state, and the sum is over excited states  $\Psi'$ . As we can see, the tiny  $\Delta E$  in the denominator will cause a considerable orbital shift which can be used to explain the large  $K_{\text{V}}$ . For  $K_{\text{Al}}$ , it can generally be interpreted by the presence of  $d$  electrons, since the Al orbital susceptibility will be enhanced to the extent that Al- $p$  orbitals participate in the relatively narrow  $d$  bands. Thus the large low- $T$  Knight shifts are consistent with a small or zero DOS at the Fermi level.

Above 250 K,  $K_{\text{Al}}$  and  $K_{\text{V}}$  are shifted to lower frequencies with rising temperature. The temperature dependence is easily understood in terms of semiconducting characteristics. Bloembergen<sup>11</sup> has calculated the Knight shift in semiconductors due to conduction electrons, which can be written as

$$K \propto T^{-1} n_e \propto \sqrt{T} e^{-E_g/2k_B T}. \quad (2)$$

Here,  $E_g$  is the gap energy of the semiconductor. The DOS in this case is assumed to be proportional to the square root of the energy near the band edge, and the Fermi energy at midgap. The carrier density  $n_e$  of the conduction electrons varies with temperature according to  $n_e \propto T^{3/2} \exp(-E_g/2k_B T)$ . The solid curves in Fig. 2 present the theoretical fits to Eq. (2) which yield energy gaps  $E_g$  of 0.21 and 0.22 eV from  $K_{\text{Al}}$  and  $K_{\text{V}}$  measurements, respectively. These are summarized in Table I.

For both  $^{27}\text{Al}$  and  $^{51}\text{V}$ , the spin shifts as fit to Eq. (2) are negative. The  $^{51}\text{V}$  spin shift is clearly due to core polarization induced by the positive spin susceptibility of vanadium  $d$  states. The  $3d$  core polarization terms are well-known to be negative.<sup>12</sup> The smaller negative  $^{27}\text{Al}$  spin shift can be attributed to coupling to  $3d$  moments via indirect interactions, which will cause a negative cross polarization of the  $s$  states.

TABLE I. Energy gap in eV deduced from the  $^{27}\text{Al}$  and  $^{51}\text{V}$  Knight shifts and  $1/T_1$ 's.

| Data         | $^{27}\text{Al}$ | $^{51}\text{V}$ |
|--------------|------------------|-----------------|
| Knight shift | 0.21             | 0.22            |
| $1/T_1$      | 0.27             | 0.28            |

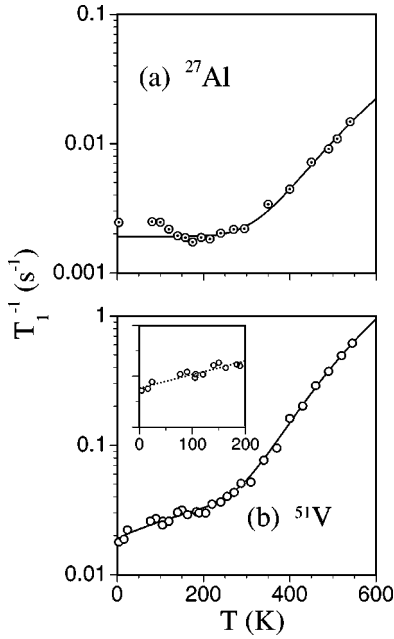


FIG. 3. Temperature dependence of relaxation rates for  $^{27}\text{Al}$  and  $^{51}\text{V}$ . Solid curves: fits to the behavior described in the text. The inset in (b) shows a linear plot of the low- $T$  relaxation rates and the dotted line represents the Korringa relaxation process corresponding to  $6.6 \times 10^{-5} \text{ s}^{-1} \text{ K}^{-1}$ .

### C. Spin-lattice relaxation rates

The temperature dependences of the spin-lattice relaxation rates ( $T_1$ 's) were measured using the inversion recovery method in the  $T$  range of 4–550 K. We recorded the signal strength by integrating the spin echo FFT of the  $^{27}\text{Al}$  ( $I=5/2$ ) and  $^{51}\text{V}$  ( $I=7/2$ ) lines. For the recovery of the  $-1/2 \leftrightarrow +1/2$  central transition, the  $T_1$ 's were extracted by fitting to different multi-exponential curves. As described above, pulse-length investigations showed the peak of both NMR lines to be  $-1/2 \leftrightarrow +1/2$  transitions. In this case, a magnetic relaxation mechanism is well known to give multi-exponential recovery for inversion recovery in NMR.<sup>7</sup> Accordingly, we have fit to the recovery curves appropriate for  $I=5/2$   $^{27}\text{Al}$  and  $I=7/2$   $^{51}\text{V}$ , with  $(1/T_1)$  as a parameter.

Figure 3 demonstrates a semilogarithmic plot of the spin-lattice relaxation rate as a function of temperature. For both  $^{27}(1/T_1)$  and  $^{51}(1/T_1)$ , there exists a large  $T$ -independent background term over the entire temperature range. A likely explanation for the nearly constant relaxation rate is the mutual interaction of local moments. This mechanism can give a  $T$ -independent contribution, as proposed by Moriya.<sup>15</sup> As evidenced by the NMR line shapes, described above, these moments must be either quite small or distributed as defects with low density.

Below 250 K the temperature dependence of  $^{27}(1/T_1)$  becomes small and a minimum was observed at about 200 K. The low- $T$  upturn in  $^{27}(1/T_1)$  cannot be attributed to independent local moments, but could be due to an incipient low-temperature phase transition, or possibly spins slowing down due to glassy behavior.<sup>14</sup> It should be noted that the mixed valance materials such as  $\text{SmB}_6$  and  $\text{YbB}_{12}$ ,<sup>15,16</sup> which exhibit characteristics of Kondo insulators, display very similar relaxation behavior accompanied by an upturn as  $T$  goes to zero. The explanation for the low-temperature

behavior was associated with localized electronic states which may spread over several atomic distances. If these localized states are destroyed with increasing temperature, the increase of  $1/T_1$  at low temperatures can possibly be interpreted by this picture.

Above 250 K,  $^{27}(1/T_1)$  rises rapidly which cannot be characterized by a normal Korringa process ( $1/T_1 \propto T$ ). Instead,  $^{27}(1/T_1)$  can be fit to the relaxation behavior in semiconductors due to conduction electrons as follows:<sup>11</sup>

$$\frac{1}{T_1} \propto \sqrt{T} n_e \propto T^2 e^{-E_g/2k_B T}. \quad (3)$$

An  $E_g$  value of 0.27 eV can be deduced and is also tabulated in Table I.

On the other hand,  $^{51}(1/T_1)$  does not have a low- $T$  upturn as in  $^{27}(1/T_1)$  but shows a Korringa relaxation process below 200 K. The resulting Korringa term is  $6.6 \times 10^{-5} \text{ s}^{-1} \text{ K}^{-1}$ , from a least-squares linear fit, shown as a dotted line in the inset of Fig. 3(b). No such Korringa process was found in  $^{27}(1/T_1)$ . These results are consistent with the band structure calculations which predicted the Fermi level DOS in  $\text{Fe}_2\text{VAl}$  to be dominated by Fe and V  $d$  electrons. Presumably, the spin dynamics causing the unusual increase in low- $T$   $^{27}(1/T_1)$  also affect the  $^{51}\text{V}$  nuclei, but are rendered unobservable by the stronger Korringa mechanism. (Note the approximately 10 times larger relaxation rates for  $^{51}\text{V}$  in Fig. 3, although the Al- $s$  hyperfine coupling is approximately 20 times larger than the V- $d$  core-polarization hyperfine coupling. The Fermi-surface weight in Al- $s$  orbitals is clearly considerably smaller than the weight in transition-metal  $d$  orbitals.)

Above 250 K,  $^{51}(1/T_1)$  deviates from the linear  $T$  dependence, exhibiting semiconductorlike behavior, as described above for  $^{27}\text{Al}$ . Note that again the rates are nearly an order of magnitude larger for  $^{51}\text{V}$ . We fit  $^{51}(1/T_1)$  to Eq. (3) added to a Korringa term extracted from the low- $T$  relaxation rates plus a constant. It is remarkable that this fits very well over the entire temperature range. The fit also gives a gap energy  $E_g$  of 0.28 eV, listed in Table I. It should be noted that the gaps deduced from the Knight shift measurements are about 20% smaller than that found in the relaxation rate data. It is possible that the discrepancy is due to an effect of the non-parabolic band edges, since an effective-mass approximation has been made in the derivation of Eqs. (2) and (3).

## III. DISCUSSION

The observed gap here is not actually a gap but rather a pseudogap with residual DOS in the Fermi level. This result is consistent with the band-structure calculations which indicate  $\text{Fe}_2\text{VAl}$  to be a semimetal,<sup>3–5</sup> with small electron and hole pockets caused by an indirect band overlap. In order to address this quantitatively, we estimate the Fermi-level DOS from the Korringa relaxation term. For  $d$ -spin relaxation in metals, the Korringa process can be represented as<sup>12</sup>

$$(T_1 T)^{-1} = 2hk_B [\gamma_n H_{hf} g(\epsilon_f)]^2 q, \quad (4)$$

where  $\gamma_n$  is the nuclear gyromagnetic ratio,  $g(\epsilon_f)$  is the  $d$ -DOS at the Fermi level,  $H_{hf}$  is the core-polarization hyperfine field, taken to be 11.7 T for vanadium,<sup>17</sup> and  $q$  is a

reduction factor equal to the reciprocal of the degeneracy.<sup>18</sup> For electron pockets located at  $X$ , as calculated for simple-cubic  $\text{Fe}_2\text{VAl}$ ,<sup>3-5</sup> the vanadium  $d$ -electron manifold has degeneracy 2 for  $e_g$  orbitals. (The  $t_{2g}$  orbitals at  $\Gamma$  which make up the hole pocket have degeneracy 3, but are dominated by Fe  $d$  states.) These parameters give  $g(\epsilon_f) = 1.7 \times 10^{-2}$  states/eV atom, for  $V$ -based  $d$  states. LMTO calculations have yielded 0.08 states/eV,<sup>5</sup> and 0.3 states/eV,<sup>3</sup> for the Fermi-level density of states in  $\text{Fe}_2\text{VAl}$ , while a calculation including gradient corrections yielded 0.1 states/eV.<sup>4</sup> Taking calculated band overlaps and hole and electron effective masses quoted by Weht and Pickett,<sup>4</sup> in the effective-mass approximation one calculates that 42% of the Fermi-level electronic states are based in  $V$ -dominated electron pockets, with the others based in a Fe-dominated hole pocket. Thus our observations correspond to a total  $V$  contribution somewhat lower, but in good general agreement, with the values calculated using band-structure methods.

Comparing to other experimental results, the observed Fermi cutoff in the photoemission studies<sup>1</sup> is consistent with the semimetallic behavior indicated on our study. The reported negative temperature coefficient of resistivity may also be attributed to a semimetal, provided the carriers that dominate the transport measurements are those in the bands removed from the Fermi level, rather than those contained in the small electron and hole pockets. Fitting the data of Nishino *et al.*<sup>1</sup> to an activated electrical conductivity yields a gap of approximately 0.1 eV, somewhat smaller than the gap we observe, of about 0.27 eV. It is not clear why these values differ, but it is possible for these to be reconciled in terms of an ordinary band gap, if the band edges are asymmetric, and nuclei interact most strongly with electrons at the conduction band edge, while at the same time the mobility of the holes is much greater, or vice versa.

As mentioned above,  $T_1$  results for  $\text{Fe}_2\text{VAl}$  are very similar to those of  $\text{SmB}_6$  and  $\text{YbB}_{12}$  which are typical Kondo lattices with an energy gap.<sup>15,16</sup> The high- $T$   $1/T_1$ 's in  $\text{SmB}_6$  and  $\text{YbB}_{12}$  have been fit to a model DOS for the  $4f$  band which consists of two rectangular peaks, separated by a small

gap with the Fermi level in the center. The proposed  $4f$  bandwidth is very narrow owing to the characteristics of  $f$  electrons. For comparison, we fit our high- $T$   $1/T_1$  results in  $\text{Fe}_2\text{VAl}$  using this model DOS, but with a wider bandwidth more reasonable for  $d$  states. The best fit yields an  $E_g$  of 0.298 and 0.242 eV from  $^{51}(1/T_1)$  and  $^{27}(1/T_1)$  data, almost the same as those obtained from Eq. (3). Hence, the NMR probe is not very sensitive to the shape of the DOS band edge in  $\text{Fe}_2\text{VAl}$ . However, in the case of  $\text{Fe}_2\text{VAl}$  this band edge is the boundary of a pseudogap containing finite carriers in the Fermi-level DOS.

There exists another class of heavy-fermion compounds also characterized as semimetals.  $\text{CeNiSn}$  is the most studied material of this type.<sup>19,20</sup> The DOS for  $\text{CeNiSn}$  is associated with a  $V$ -shaped pseudogap bounded by two sharp narrow peaks with a finite number of carriers at the Fermi level. For a material with such a DOS, the  $1/T_1$  is proportional to  $T^3$  at low temperatures, but shows  $T$  dependence characteristic of an ordinary gap at high temperatures. As we can see from the inset in Fig. 3(b),  $\text{Fe}_2\text{VAl}$  does not indicate such behavior.

#### IV. CONCLUSIONS

In summary, the microscopic electrical properties of  $\text{Fe}_2\text{VAl}$  have been studied in detail in  $^{27}\text{Al}$  and  $^{51}\text{V}$  NMR. The results of Knight shifts as well as spin lattice relaxation rates appear to be easily understood in terms of semimetallic characteristics for  $\text{Fe}_2\text{VAl}$ . From the relaxation behavior we deduce the Fermi-level DOS to be a relatively small value, in agreement with band-structure calculations. The unusual upturn in  $^{27}(1/T_1)$  at low temperatures still remains to be explained, and we plan further investigation of the behavior in this region.

#### ACKNOWLEDGMENTS

We are grateful to D. G. Naugle and V. Iyer for help with sample preparation. This work was supported by Texas A&M University.

\*Electronic address: c019877@unix.tamu.edu

†Electronic address: jhross@tamu.edu

<sup>1</sup>Y. Nishino *et al.*, Phys. Rev. Lett. **79**, 1909 (1997).

<sup>2</sup>Z. Fisk *et al.*, Science **239**, 33 (1988).

<sup>3</sup>D. J. Singh and I. I. Mazin, Phys. Rev. B **57**, 14 352 (1998).

<sup>4</sup>Ruben Weht and W. E. Pickett, Phys. Rev. B **58**, 6855 (1998).

<sup>5</sup>G. Y. Guo, G. A. Botton, and Y. Nishino, J. Phys. Condens. Matter **10**, L119 (1998).

<sup>6</sup>J. W. Allen, B. Batlogg, and P. Wachter, Phys. Rev. B **20**, 4807 (1979).

<sup>7</sup>Chin-Shan Lue, Suchitra Chepin, James Chepin, and Joseph H. Ross, Jr., Phys. Rev. B **57**, 7010 (1998).

<sup>8</sup>O. Kanert and M. Mehring, *NMR: Basic Principles and Progress*, edited by E. Fluck and R. Kosfeld (Springer-Verlag, New York, 1971), Vol. 3, p. 1.

<sup>9</sup>C. Kittel and Elihu Abrahams, Phys. Rev. **90**, 238 (1953).

<sup>10</sup>C. P. Slichter, *Principles of Magnetic Resonance* (Springer-Verlag, New York, 1990).

<sup>11</sup>N. Bloembergen, Physica **20**, 1130 (1954).

<sup>12</sup>*Metallic Shifts in NMR*, edited by G. C. Carter, L. H. Bennett, and D. J. Kahan (Pergamon, Oxford, 1977).

<sup>13</sup>Toru Moriya, *Spin Fluctuations in Itinerant Electron Magnetism* (Springer-Verlag, Berlin, 1985).

<sup>14</sup>D. Bloyet *et al.*, Phys. Rev. Lett. **40**, 250 (1978).

<sup>15</sup>M. Takigawa *et al.*, J. Phys. Soc. Jpn. **50**, 2525 (1981).

<sup>16</sup>M. Kasaya, F. Iga, M. Takigawa, and T. Kasuya, J. Magn. Magn. Mater. **47-48**, 429 (1985).

<sup>17</sup>B. N. Ganguly, Phys. Rev. B **8**, 1055 (1973).

<sup>18</sup>Y. Yafet and V. Jaccarino, Phys. Rev. **133**, A1630 (1964).

<sup>19</sup>K. Nakamura *et al.*, Physica B **206&207**, 829 (1995).

<sup>20</sup>Ko-ichi Nakamura *et al.*, Phys. Rev. B **54**, 6062 (1996).